Assessment of Floor Heave Associated with Bumps in a Longwall Mine Using the Discrete Element Method

Bo Hyun Kim
Mark K. Larson
Mine Safety Branch, Spokane Mining Research Division, CDC/NIOSH

ABSTRACT

This study was developed as part of an effort by the National Institute for Occupational Safety and Health (NIOSH) to better understand rock-mass behavior in longwall coal mines in highly stressed, bump-prone ground. The floor-heave and no-floor-heave phenomena at a western U.S. coal mine cannot be properly simulated in numerical models using conventional shear-dominant failure criteria (i.e., Mohr-Coulomb or Hoek-Brown failure criterion). Kim and Larson (2019) demonstrated these phenomena using a user-defined model of the s-shaped brittle failure criterion in conjunction with a spalling process in FLAC3D. The results of the FLAC3D modeling agreed with the observations of the relative amounts of heave from each gate-road system. However, the FLAC3D model adopted many assumptions and simplifications that were not very realistic from a physical or mechanical perspective. In order to overcome the limitations of the FLAC3D model, 3DEC modeling in conjunction with the Discrete Fracture Network (DFN) technique was performed to better understand the true behavior of floor heave associated with underground mining in an anisotropic stress field. The effect of stress rotation in the mining-induced stress field was considered by using a different geometry of rock fractures in the coal seam. The heterogeneity of the engineering properties (i.e., cohesion and tensile strength) were also considered by using Monte Carlo simulations. Consequently, the 3DEC models using the DFN technique resulted in predictions of floor heave that agreed with observations of the relative amounts of heave from each gate-road system, but the cause of heave was mainly related to the degree of anisotropy instead of the size of the pillar.

INTRODUCTION

Floor failure in coal mines often inhibits longwall mining operations, as large displacement of floor strata, known as floor heave, interferes with travel, access, ventilation, and equipment operation. This study was developed as part of an effort by the National Institute for Occupational Safety and Health (NIOSH) to better understand rock-mass behavior in longwall coal mines in highly stressed, bump-prone ground.

NIOSH researchers observed floor heave at a western U.S. coal mine where pillar width in a three-entry gate-road system was 52 m, whereas no perceptible floor heave occurred where the pillar width in the gate-roads was 22 m (Lawson 2015). The floor heave most often occurred soon after development, and additional stress resulting from panel mining only increased the amount of floor heave. In addition, regular face and butt cleat systems were observed in the seam throughout the gate-roads with smaller pillars, but they were variable in orientation in the seam in the gate roads with larger pillars, particularly in areas within 200 m of intersecting faults. This area of irregular cleat orientation is of particular interest because a bump later occurred with damage that included much of this area with variable cleats.

Mine engineers at two nearby mines reported the same correlation of floor heave with larger pillars, and such heave was not avoided by designing with empirical tools. The authors have personal knowledge of floor heave associated with large pillars at another mine in a different western coalfield. Mining-induced seismic events are prevalent to varying degrees at these mines. Floor heave and bumps are often associated with one another, regardless of the bump mechanism.

Kim and Larson (2019) attempted to explain, through numerical models, small energy releases in the form of floor heave. They claimed that brittle rock failure is associated with both floor heave and some bump mechanisms, if not directly involved in their cause. They also demonstrated the floor-heave/no-floor-heave phenomenon associated with pillar width changes using a user-defined model of the s-shaped brittle failure criterion in conjunction with a spalling process in FLAC3D. The results of the FLAC3D modeling agreed with the observations mentioned earlier of relative amounts of heave from each gate-road system.

However, the FLAC3D model adopted many assumptions and simplifications that were not very realistic from a physical or mechanical perspective. In order to overcome the assumptions

and simplifications of the FLAC3D model, in this study, 3DEC (Itasca Consulting 2019) modeling in conjunction with the Discrete Fracture Network (DFN) technique was performed to better approximate the true behavior of floor heave associated with underground mining in an anisotropic stress field. The effect of stress rotation in a mining-induced stress field was considered by rotating the excavation and DFN with respect to the loading directions. The heterogeneity of the engineering properties (i.e., cohesion and tensile strength) was also considered by using Monte Carlo simulations.

Thus, there are two main goals of this study. First, to construct different levels of anisotropy and different cleat systems with DFNs in 3DEC. Second, to test these models to see if they can replicate the floor-heave and no-floor-heave phenomena and explain the influence of anisotropy and cleat development on the failure mechanisms in each gate-road system. In this study, the DFN is used to attempt to explicitly create the different levels of anisotropy and development of cleat sets in the coal seam of each gate-road system. A contrasting statistical parameter is used for the realization of the DFNs. As a result, the poorly-cleated coal seam with oblique angles from horizontal— where horizontal is the plane that is parallel to the simulated coal seam —is generated in the wide pillar system, and the well-cleated coal seam with sub-parallel angles from horizontal is generated in the narrow pillar system, respectively. Ultimately, 3DEC analyses in conjunction with the DFNs are shown to replicate the floor-heave and no-floor-heave phenomena previously simulated using FLAC3D models (Kim and Larson (2019)), and explains the influence of anisotropy and cleat development on the failure mechanism in each gate-road system.

The next section discusses cleats in coal seams and their impact on the mechanical behavior of coal. Then, the following section describes the approach used for the laboratory testing, including sample preparation, and loading conditions used. Finally, the approaches for examining strength as a function of orientation between cleat and loading direction are explained and these results are compared to analytical and numerical analysis results. Spatial characteristics of coal cleats

Fractures occur in nearly all coal beds and can exert fundamental control on coal stability, minability, and fluid flow. As illustrated in Figure 1, cleats are fractures that usually occur in two sets that are, in most instances, mutually perpendicular and also perpendicular to bedding (Laubach et al. 1998).

Generally, cleats occur with spacing on a scale of only 1–6 cm. Many researchers have found and reported that the spatial characteristics of cleats in terms of their angle to the greatest compressive principal stress direction control not only global strength, but also impact the relative brittleness of the coal. Agapito and Goodrich (2000) reported that Western U.S. dynamic failure events are associated with coals that are poorly cleated, indicating wider-than-usual spacing between cleat apertures. Hebblewhite and Galvin (2016) noted localized variability in cleat distribution in conjunction with the location of the double fatality coal burst at the Austar mine in Australia in 2014. In addition, the resultant anisotropy is influenced by the geometric relationship between the direction of mine development and the orientation of in-situ stress. More recently, Kim and Larson (2017) and Kim et al. (2018) found that cleats play a significant role in determining anisotropy

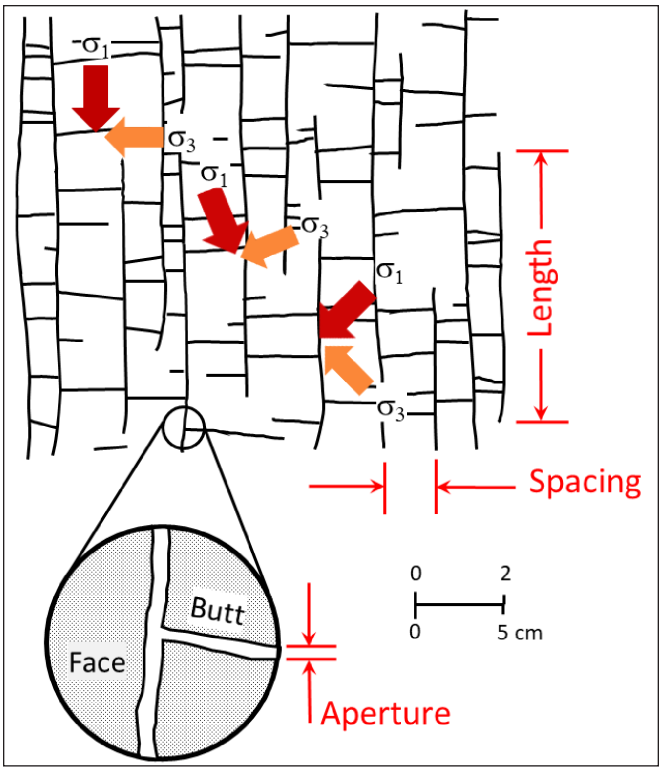

Figure 1. Cleat hierarchies in cross-section view (after (Laubach et al. 1998)).

of strength and brittleness. The results also showed that the numerical specimen exhibited one of the weakest strengths but the most brittle Hoek-Brown constants (m_i) when the cleat was oriented at 30 degrees from the axial loading direction. Therefore, the included angle between the principal stresses (as illustrated by the arrows in Figure 1) and orientation of the cleats governs the anisotropic strength and behavior of a coal.

3DEC AND DFN SIMULATIONS FOR ASSESSMENT OF FLOOR HEAVES

Preparation of a 3DEC Model

A model with dimensions of 480(W) × 370(H) × 10(L) m was constructed as illustrated in Figure 2. Based on the field observation by Lawson (2015), the immediate floor in the wide pillar and in the narrow pillar were considered as more anisotropic and less anisotropic material, respectively.

It was also considered that the heights of each layer of rock mass in the model are 182 m for the top, 4 m for the seam and the floor, and 178 m for the bottom layer, respectively. The depth of the top boundary of the model from the surface was set at 474.4 m below the surface (top-of-seam 656.4 m below surface). A surcharge of vertical stress was applied on the top boundary of the model to account for the weight of overburden not explicitly represented in the model. The horizontal stresses were considered to be greater than the vertical stress. It was presumed that the major principal stress (σ_H) had a magnitude (MPa) of 3.5 × overburden stress in the y-direction of the model. The intermediate principal stress (σ_h) had a magnitude (MPa) of 2.5 × overburden stress in the *x*-direction of

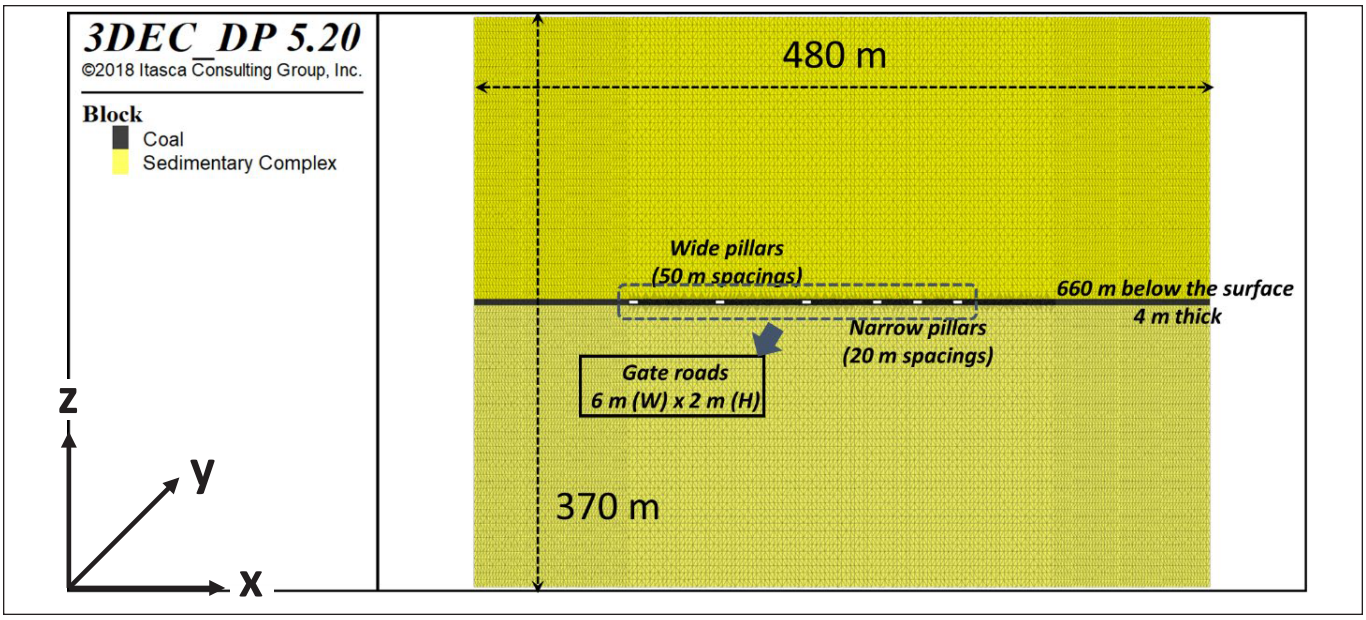

Figure 2. Layout of the 3DEC model (not to scale).

the model. The minor principal stress (σ_v) had a magnitude (MPa) of the unit weight × depth (Kim and Larson 2019).

For the boundary conditions, both sides of the model were fixed in the x-direction, and both the front and back of the model were fixed in the y-direction. The bottom of the model was fixed in the z-direction. The geometries of the gate-roads and pillars were simplified so that the gate-road entries were 6-m wide and 4-m high, leaving pillars that were 22-m and 52-m wide. The equivalent zone size of the individual mesh elements in the model was set as 1 m for both the top and bottom layer of rock mass and as 0.5 m for the seam and floor, respectively.

Realization of Cleats and Bedding Planes in the Coal Seam Using DFNs

Lawson (2015) observed and confirmed that the orientation of cleating in the region of the wide pillars system showed a zone of localized deviation from the norm with respect to both spacing and orientation. While faulting also is noted in the area, the distribution of cleat orientation near the fault has not been quantitatively measured but has been visually estimated. This zone of cleats with variable orientation by the fault is extended for a distance of several pillars—far beyond the spatial extent of the mapped fault plane. Similar observations were made by Robeck (2005), who noted changes in cleat characteristics for a distance exceeding 30 m from visible fault planes.

The changes noted by Lawson et al. (2012) correlated with an associated zone of anomalous deterioration observed over a period of time, preceding a large-scale seismic event. Although not observable, it is assumed that the cleating extended into the floor because it was composed of coal and carbonaceous mudstone (Lawson 2015). Similar changes in cleat characteristics were not observed in the gate-road with narrow pillars. It is, therefore, anticipated that the orientation of cleats to the loading direction driven by the major principal stress, the so-called included angle, would control the anisotropic behavior.

In this section, the built-in DFN generator in 3DEC is used to explicitly realize the spatial anisotropic characteristics of the coal seam observed from a bump-prone underground coal mine. The spatial characteristics of the discontinuities (i.e., cleats and bedding planes) as input data for the 3DEC model are estimated based on the results of the laboratory tests and field observations.

The different dip angles of the bedding planes were used to generate the DFNs that more explicitly represent two anisotropies of coal in a 480(W) × 4(H) × 10(L) m numerical domain. Two sets of bedding planes are presented in this section, having mean dip angles of s0° and 30° from horizontal—where horizontal is the direction parallel with the seam.

The orientations of the cleats and bedding planes are plotted in a stereographic projection as shown in Figure 3. The Fisher distribution based on these orientations is used to generate the DFNs. The Power-law distribution is chosen to determine the sizes of the cleats (0.01 m to 0.1 m) and the bedding planes (100.0 m to 500.0 m), respectively. The generated DFNs are illustrated in Figure 4.

Stochastic Approach for Considering Heterogeneity Of Engineering Properties by Monte Carlo Simulation

All blocks in the 3DEC model are built as deformable and elastic blocks. The DFNs are created only in the coal seam in the model. The heterogeneity of the engineering properties (i.e., cohesion and tensile strength) in the 3DEC models is also considered using Monte Carlo simulations. The heterogeneous strengths can be modeled by populating the blocks and block contacts of the model with probability distributions. In the 3DEC models, the blocks

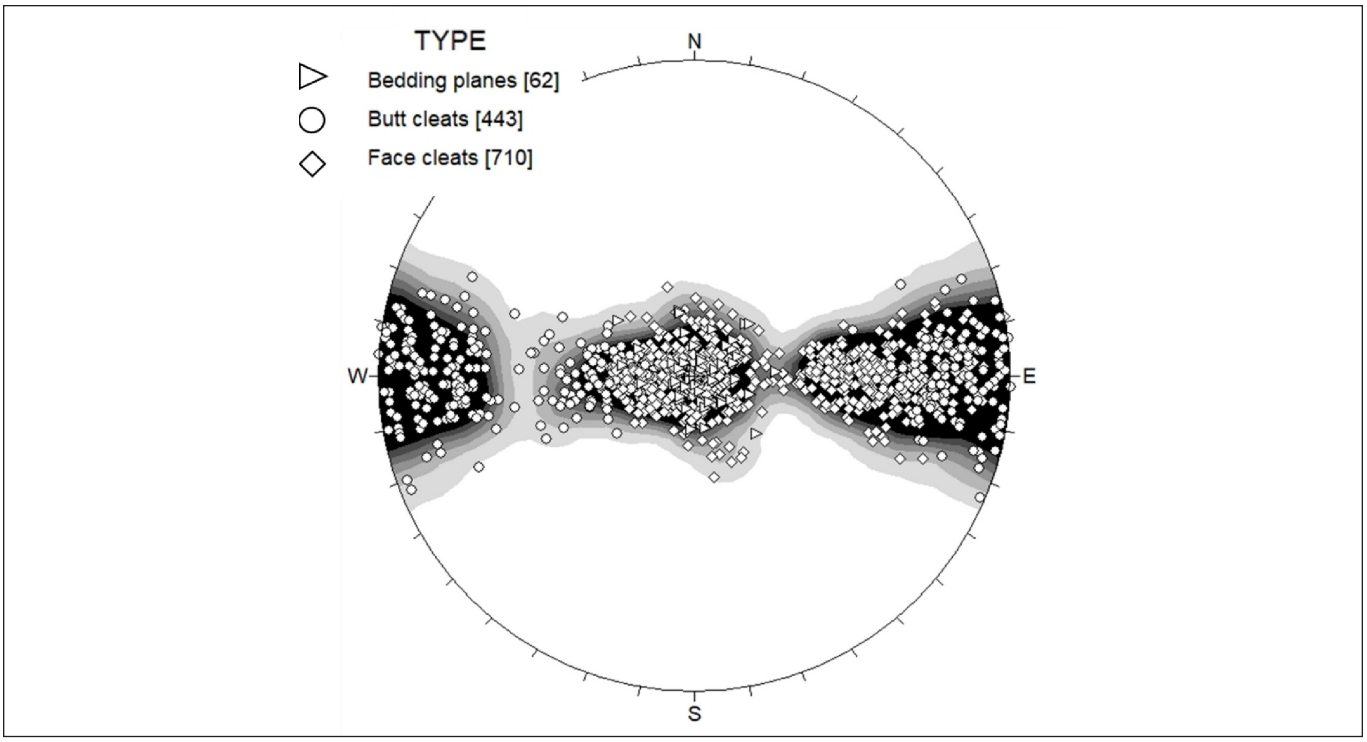

Figure 3. The orientations of the cleats and bedding planes are plotted in a stereographic projection.

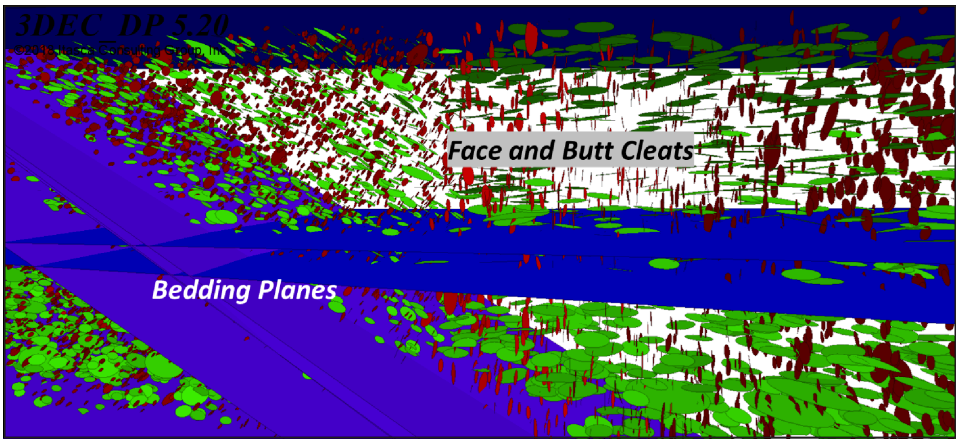

Figure 4. Face and butt cleats (red and green disks) perpendicular to bedding planes (blue planes) created by the DFNs.

are defined as elastic and zones formed with an approximate edge length of 0.1 m. The built-in Mohr C++ plug-in is used in the models. In order to create the numerical specimens, each block contact is assigned a cohesion and a tensile strength value randomly selected from the probability distributions generated by the Monte Carlo simulation as shown in Figure 5. The range of the cohesion and the tensile strength is 1.35±0.91 MPa and 0.45±0.30 MPa, respectively. All sub-contacts forming each contact are assigned the same tensile strength and cohesion.

Figure 5 shows the cumulative distributions of the cohesion and tensile strength, (a) and (b), and the assigned properties in the coal seam in the 3DEC model (c).

Table 1 shows the input data used for the 3DEC model. The material properties are estimated based on the results of laboratory tests (Kim et al. 2018) and field observation (Lawson 2015), and the literature (Farmer 1968; British Geological Survey 2002; Tesarik et al. 2013). Ten different 3DEC models were constructed, each having a different realization of DFN generation.

RESULTS AND DISCUSSION

Kim and Larson (2019) conducted the FLAC3D modeling such that where the open joints controlling rock-mass strength had a preferred orientation, ubiquitous joints (UBJ) were activated within the model with orientations that reflect the true orientation distribution. This approach, referred to as the Ubiquitous Joint Rock

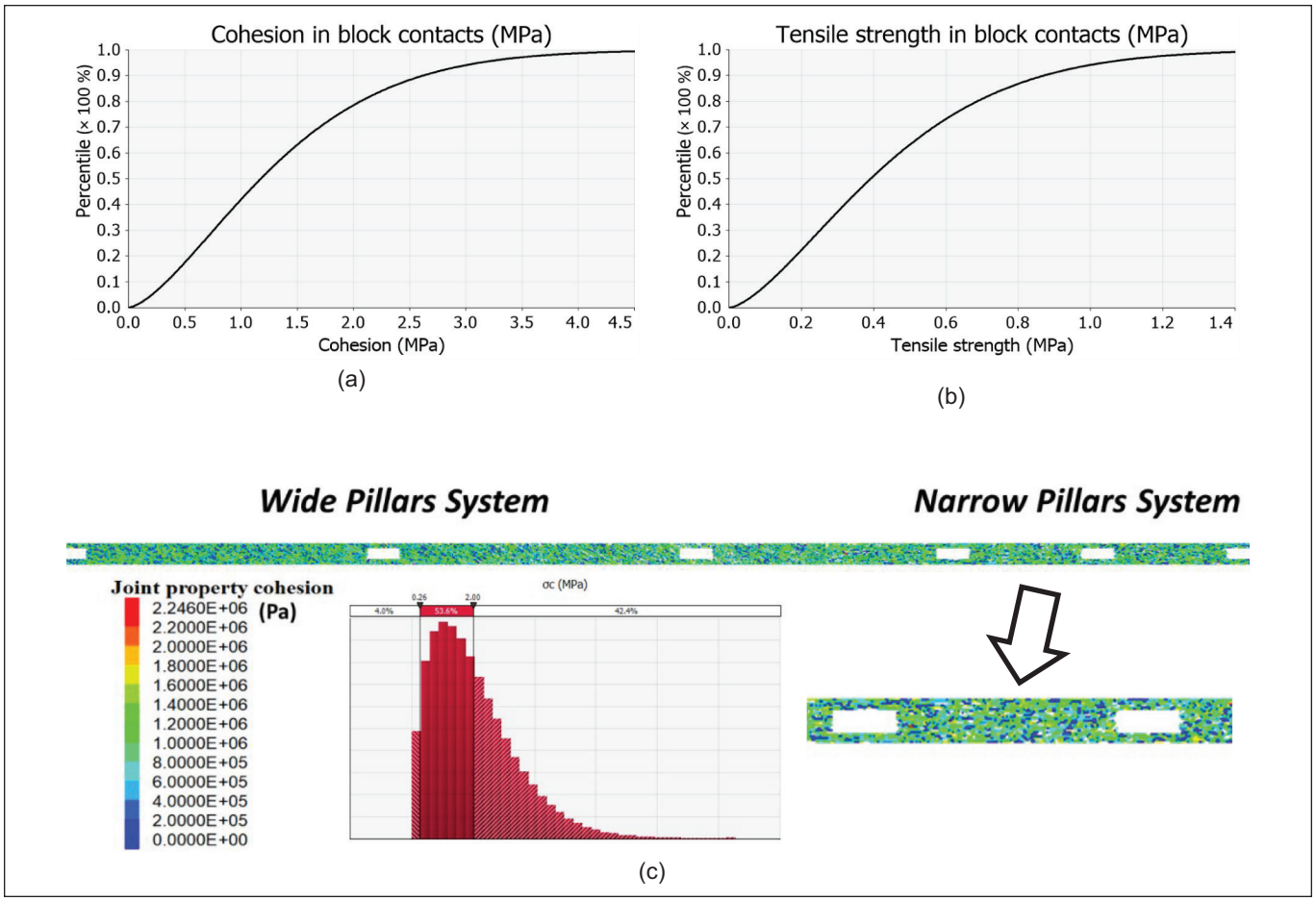

Figure 5. The probability distributions generated by the Monte Carlo simulation [(a) cohesion and (b) tensile strength] and (c) the assigned cohesion (histogram: distribution of the cohesion) for (sub-)contacts of blocks in the 3DEC model.

Table 1. Input data for the seam and the surrounding rocks in the 3DEC model

Zone Group	Young's Modulus (GPa)	Poisson's Ratio	Joint Properties					Remark [3DEC (Itasca Consulting Group 2016)]
			Normal Stiffness (GPa/m/m)	Shear Stiffness (GPa/m/m)	Cohesion (MPa)	Friction Angle (°)	Tensile Strength (MPa)	
Seam 3.8		0.25	105	52.5	1.35 (±0.91)	35	0.45 (±0.30)	Mohr model
Top	20.7	0.2	—	—	—	—	—	Elastic model
Bottom	9.8	0.25	—	—	—	—	—	Elastic model

Mass (UJRM) model, originally was conceived by Clark (2006) as a means to account for the impact of jointing on rock-mass strength more explicitly within FLAC3D by assigning a unique joint orientation to each zone. Since then, it has been extended and applied in FLAC3D to the study of cave propagation (Pierce et al. 2006; Sainsbury et al. 2008; Board and Pierce 2009). Introduction of ubiquitous joints in this manner implicitly introduced scale effects, anisotropy, and variability.

To be clear, in the FLAC3D model, Kim and Larson (2019) treated the material properties differently in the wide pillar system than in the narrow pillar system. This assumption was developed based on the laboratory testing results. Specifically, the material properties in the wide pillar system had lower strength and greater brittleness than the properties in the narrow pillar system. This implicit approach permitted replication of the different developing cleating systems in the coal seam that was previously observed (Lawson 2015).

Kim and Larson (2019) also found that the dip angles of the simultaneously installed ubiquitous joints are more or less oblique within the range from 20° to 40° relative to horizontal in the wide pillar system. However, the dip angles can be found as sub-horizontal ubiquitous joints (UBJ) (< 10°) adjacent to the floor or sub-vertical

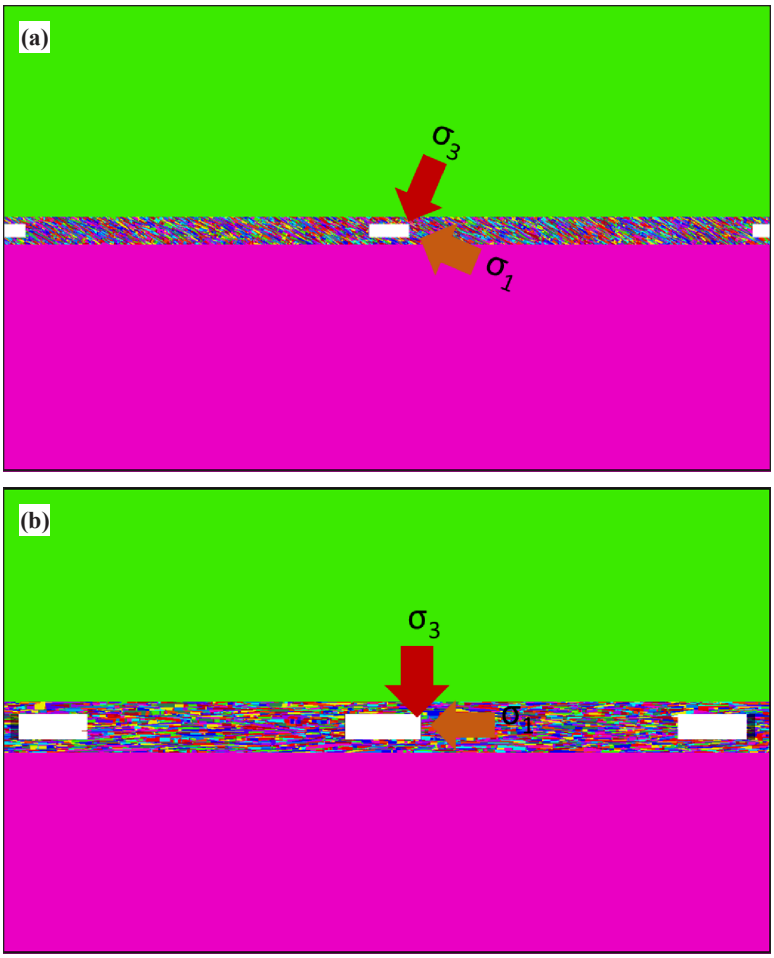

Figure 6. Introduced discrete fracture networks for cleats and bedding planes in the vicinity of gate-roads in (a) wide pillars and in (b) narrow pillars.

UBJ (> 80°) adjacent to the ribs of gate-roads in the narrow pillar system. In this study, the coal properties were kept the same between the narrow and wide pillar systems. Greater anisotropy for the wide pillar system was achieved, instead, by the explicit introduction of DFNs, with the wide pillar system having a wider range of orientation and smaller spacing and persistence than in the narrow pillar system, where DFNs had a smaller range of orientation that was sub-horizontal or sub-vertical.

Figure 6 presents the rock blocks consisting of cleats and bedding planes in the coal seam explicitly created by the DFN technique. We conducted 10 realizations of the DFN to construct the cleats system in the coal seam. The largely dispersed poles in the stereographic projection as shown in Figure 3 indicate the orientation of the DFN in the wide pillar system. The congregated poles in the stereographic projection as illustrated in Figure 3 present the orientation of the DFNs in the narrow pillar system. Figure 6(a) shows the blocky coal seam in the wide pillar system where the dip angles of the mean bedding planes are assumed to be 30° from horizontal. Figure 6(b) illustrates the blocky coal seam in the narrow pillar system where the dip angle of the mean bedding plane is horizontal. The cleats in the wide pillar system, as shown in Figure 6(a), are realized by DFNs with approximately 20% less fracture frequency and cleats half the size of the cleats in the narrow pillar system as illustrated in Figure 6(b). These features produce a relatively poorly cleated coal seam by the less persistent cleats in the wide pillar system but produce a relatively well-cleated coal seam by the more persistent cleats in the narrow pillar system. In this way, the included angle between the principal stresses, as illustrated by the arrows in Figure 6, and cleat orientations govern the anisotropic strength and behavior of the coal.

The contours of the displacements around the gate-roads are presented in Figure 7. The red contours indicate total displacements greater than 20 cm. This value is equivalent to 10% of the height of the gate-road. In the wide pillar system, as shown in Figure 7, the displacement contours are developed deeper and more localized, whereas the displacement contours in the narrow pillar system show shallow and uniform distributions. This result occurs because of the different degree of anisotropy represented by the different dips of the DFNs, as explained earlier.

Figure 7(b) and Figure 7(c) more closely illustrate the deformation around the boundary of the gate-road in the wide pillar system and the narrow pillar system, respectively. The maximum displacement measured on the floor of the gate-road in the wide pillar system is

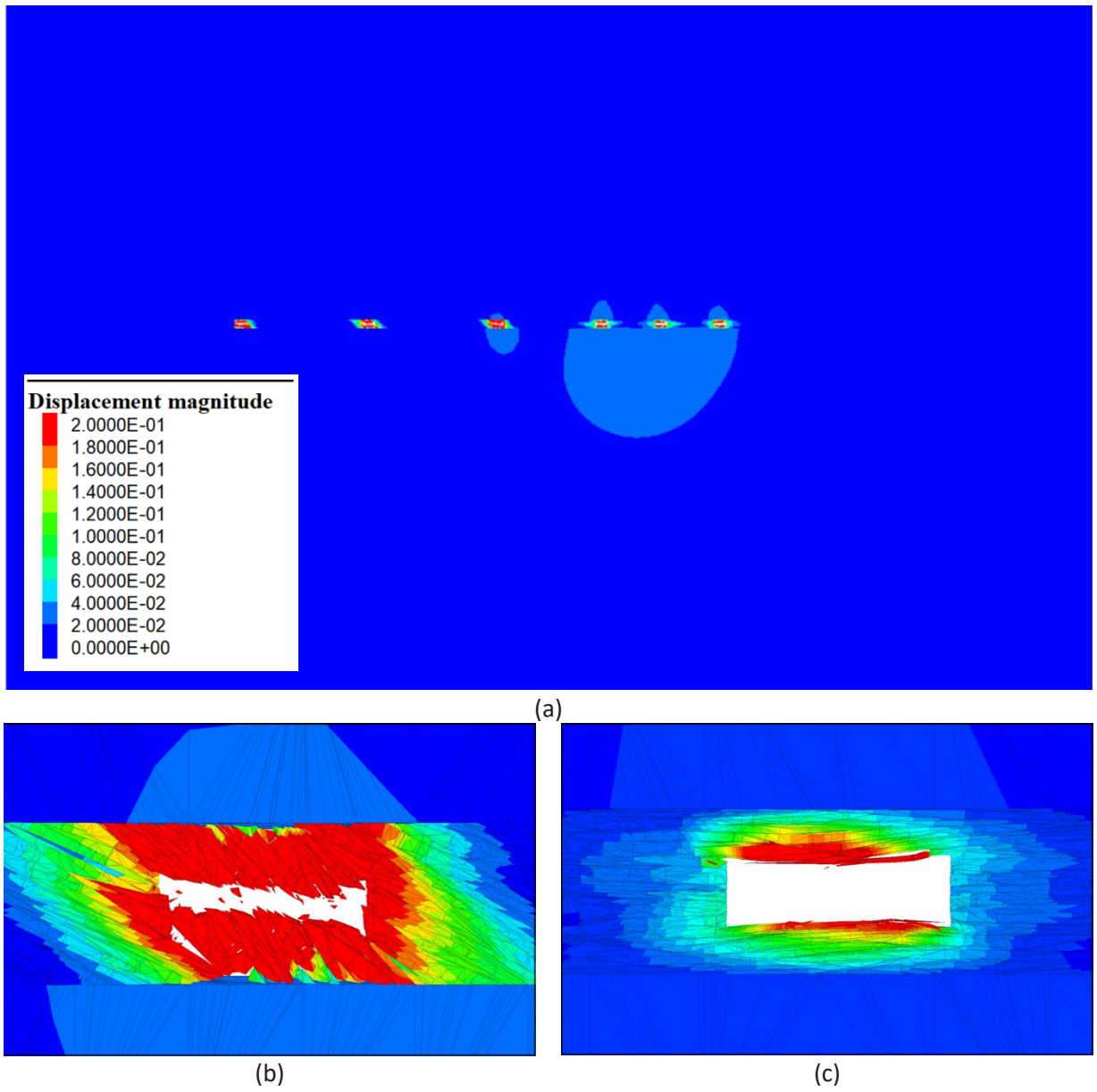

Figure 7. (a) The contours of displacement calculated in the 3DEC model, (b) the contours of displacement and profile of deformation of the gate-road in the wide pillar system, and (c) the contours of displacement and profile of deformation of the gate-road in the narrow pillar system.

about 0.35 m. The maximum displacement measured on the floor of the gate-road in the narrow pillar system is about 0.014 m.

Figure 8 presents the contours of maximum shear strain increments associated with the dissipated plastic energy. The maximum contour was cutoff at 0.2 m/m, but the maximum shear strain increment in the wide pillar system was much higher than that amount. Therefore, the maximum shear strain increments are developed more extensively in the wide pillar system, Figure 8(a), than in the narrow pillar system, Figure 8(b).

In summary, we have presented the DFN technique for implementing models having different anisotropic characteristics in the floor and coal of the narrow pillar region and the wide pillar region. The results of the numerical modeling matched observations of the relative amounts of heave from each gate-road system.

CONCLUSION

A numerical simulation for understanding the true behavior of a rock mass associated with underground mining was conducted by researchers from the National Institute for Occupational Safety and Health (NIOSH).

3DEC modeling in conjunction with the DFN technique was performed to better understand the true behavior of a floor heave associated with underground mining in the anisotropic stresses field.

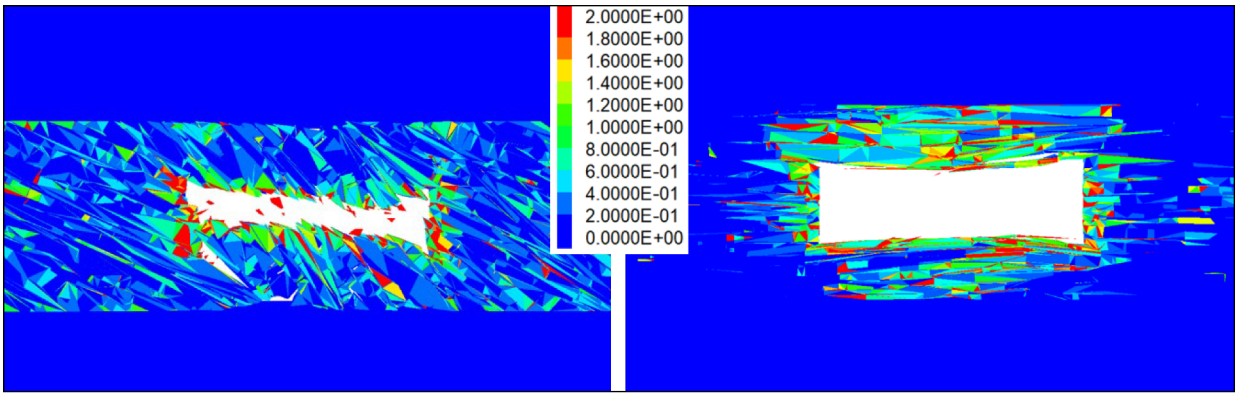

Figure 8. (a) The contours of maximum shear strain increments around the gate-road in the wide pillar system, and (b) the contours of maximum shear strain increments around the gate-road in the narrow pillar system.

The effect of stress rotation in the mining-induced stress field was considered by using different means of DFN orientation distribution in the coal seam. The wide pillar system had an oblique included angle that was generated by the DFN with a higher variability of the orientations. The narrow pillar system had a normal included angle that was generated by the DFN with a lower variability of the orientations.

The spatial characteristics of the discontinuities (i.e., cleats and bedding planes) as input data for the 3DEC model were estimated based on the results of the laboratory tests and the field observation. The DFNs explicitly simulated poorly and well cleated coal seams, indicating the different spacing between cleat apertures using the probability distribution functions on fracture density (or frequency) and size. The heterogeneity of the engineering properties (i.e., cohesion and tensile strength) were also considered by the Monte Carlo simulations.

The 3DEC models using the DFN technique demonstrated that the results of the modeling agreed with the observations of the relative amounts of heave from each gate-road system. The results represent a more realistic improvement compared to the implicit approach used with the FLAC3D model. The natural fractures in coal, cleats, are very significant regarding the coal's anisotropy of strength and brittleness.

We conclude that such characteristics can explain the observed phenomenon of floor heave associated with the larger pillars and no significant floor heave associated with the smaller pillar system.

DISCLAIMER

The findings and conclusions in this report are those of the author(s) and do not necessarily represent the official position of the National Institute for Occupational Safety and Health. Mention of any company or product does not constitute endorsement by NIOSH.

REFERENCES

Agapito, J. F. T., and Goodrich, R. R. 2000. Five stress factors conducive to bumps in Utah, USA, coal mines. In *Proceedings: 19th International Conference on Ground Control in Mining*. Peng, S. S., and Mark, C. eds. (Morgantown, WV: August 8–10, 2000) Morgantown, WV: West Virginia University, pp. 93–100.

Board, M., and Pierce, M. E. 2009. A review of recent experience in modeling of caving. In *Proceedings of the International Workshop on Numerical Modeling for Underground Mine Excavation Design*. Esterhuizen, G. S.*, et al.* eds. NIOSH Information Circular 9512, (Asheville, NC: June 28, 2009) Pittsburgh, PA: U.S. Department of Health and Human Services, National Institute for Occupational Safety and Health (NIOSH), pp. 19–28.

British Geological Survey 2002. *Engineering geology of British rocks and soils, mudstones of the Mercia Mudstone Group, Urban Geoscience and Geological Hazards Programme*. Research Report RR/01/02, 106 pp.

Clark, I. H. 2006. Simulation of rockmass strength using ubiquitous joints. In *Proceedings of the 4th International FLAC Symposium on Numerical Modeling in Geomechanics*. Hart, R., and Varona, P. eds. (Madrid, Spain: May 29–31, 2006) Minneapolis, MN: Itasca Consulting Group, Inc.

Farmer, I. W. 1968. *Engineering properties of rocks* (London: E. & F. N. Spon), 180 pp.

Hebblewhite, B., and Galvin, J. M. 2016. A review of the geomechanics aspects of a double fatality coal burst at Austar Colliery in NSW, Australia in April 2014. In *Proceedings: 35th International Conference on Ground Control in Mining*. Barczak, T.*, et al.* eds. (Morgantown, WV: July 26–28, 2016) Morgantown, WV: West Virginia University, pp. 140–145.

Itasca Consulting, G., Inc., 2019. 3DEC distinct element modeling of jointed and blocky material in 3D. User's guide. version 7.0. Itasca Consulting Group, Inc.,. http://docs.itascacg.com/3dec700/3dec/docproject/source/3dechome.html.

Itasca Consulting Group, I. 2016. *3DEC: 3-dimensional universal Distinct Element Code, version 5.2, user's manual* (Minneapolis: Itasca Consulting Group, Inc.).

Kim, B.-H., and Larson, M. K. 2019. Numerical investigation of factors involved in a floor heave mechanism in a bump-prone coal mine. In *Proceedings of the 38th International Conference on Ground Control in Mining*. Klemetti, T.*, et al.* eds. (Morgantown, WV: July 23–25, 2019) Englewood, CO: Society for Mining, Metallurgy, and Exploration, Inc. (SME),, pp. 93–101.

Kim, B.-H., Walton, G., Larson, M. K., and Berry, S. 2018. Experimental study on the confinement-dependent characteristics of a Utah coal considering the anisotropy by cleats. *Int. J.*

Rock Mech. Min. Sci., 105: 182–191, https://doi.org/10.1016/j.ijrmms.2018.03.018.

Kim, B. H., and Larson, M. K. 2017. Evaluation of bumps-prone potential regarding the spatial characteristics of cleat in coal pillars under highly stressed ground conditions. In *Proceedings, 51st U.S. Rock Mechanics/Geomechanics Symposium.* (San Francisco: June 25–28, 2017) Alexandria, VA: American Rock Mechanics Association (ARMA), 8 pp.

Laubach, S. E., Marrett, R. A., Olson, J. E., and Scott, A. R. 1998. Characteristics and origins of coal cleat: A review. *Int. J. Coal Geol.,* 35(1–4): 175–207, http://dx.doi.org/10.1016/S0166-5162(97)00012-8.

Lawson, H. E. 2015. Verbal conversation between Heather Lawson and Larson, M. K., July 29.

Pierce, M., Cundall, P., Ivars, D. M., Darcel, C., Young, R. P., and Reyes-Montes, J. 2006. *Six monthly technical report, caving mechanics, Sub-Project No. 4.2: Research and metholodogy improvemenet, and Sub-Project 4.3: Case study application*. Report to Mass Mining Technology Project. Minneapolis, MN: Itasca Consulting Group.

Robeck, E. D. 2005. *The effects of fault-induced stress anisotropy on fracturing, folding and sill emplacement: Insights from the Bowie Coal Mines, Southern Piceance Basin, western Colorado*. (M.S. thesis), Brigham Young University. 106 pp.

Sainsbury, B., Pierce, M., and Mas Ivars, D. 2008. Simulation of rock mass strength anisotropy and scale effects using a Ubiquitous Joint Rock Mass (UJRM) model. In *Continuum and Distinct Element Numerical Modeling in Geo-Engineering — 2008, Proceedings of the 1st International FLAC/DEM Symposium*. Hart, R. D.,Detournay, C. L., and Cundall, P. A. eds. (Minneapolis, MN: August 25–27, 2008) Minneapolis, MN: Itasca Consulting Group, Inc., pp. 241–250.

Tesarik, D. R., Whyatt, J. K., and Larson, M. K. 2013. Inferring mine floor properties from pillar size and floor heave. In *Proceedings of the 47th U.S. Rock Mechanics/Geomechanics Symposium*. Pyrak-Nolte, L. J*., et al.* eds. (San Francisco, CA: June 23–26, 2013) Alexandria, VA: American Rock Mechanics Association, pp. 438–450.